# Supplementary Information

## Novel [$BO_2$] Superhalogen Module-Enabled Deep-ultraviolet Nonlinear Optical Material: Rational Design for Tailored Birefringence and Phase Matching

Aqsa Munawar,[a][b]# Abudukadi Tudi,[a]# Ke Li,[a] Changyou Liu,[a] Zhihua Yang [a][b]* and Shilie Pan [a][b]*

[a] Research Center for Crystal Materials; State Key Laboratory of Functional Materials and Devices for Special Environmental Conditions; Xinjiang Key Laboratory of Functional Crystal Materials; Xinjiang Technical Institute of Physics and Chemistry, Chinese Academy of Sciences, 40-1 South Beijing Road, Urumqi 830011, P.R. China;

[b] University of Chinese Academy of Sciences, Beijing 100039, P.R. China.

[#] A. Munawar, A. Tudi, contributed equally to this work.

*Corresponding authors : zhyang@ms.xjb.ac.cn (Zhihua Yang), slpan@ms.xjb.ac.cn (Shilie Pan)

**Calculation Methodologies**

Looking back to the invention of KBBF, the *ab initio* algorithm joined with anionic group theory proves an effective way to insight study of the optical properties of anionic moiety in crystals.[1] The DFT-energy band approach was carried out to calculate the macroscopic coefficient of SHG through high performance computer.[2,3] Literature study reveals that the first principle calculations got remarkable achievement to obtain the NLO properties and elucidate the relationship among the microstructure and macro-NLO properties. As compared to the conventional empirical approach that requires much time, trial along with error, researchers are agreed to subsume themselves in convenient, controllable, efficient efforts to design and search novel functional NLO structures. To fulfill these objectives, a theoretical approaches offer efficiently to evaluate and determine the DUV-NLO performance including band energy gap, SHG coefficient, birefringence and phase matching output wavelength of designed NLO crystals.

**Accurate Band Gap Evaluation**

The system energy was treated iterated till a tolerance of $2 \times 10^{-7}$ eV/atom was achieved for electronic relaxation. The Monkhorst Pack k point meshes in the Brillouin zone was set as $3 \times 3 \times 3$ for $CsBe_2B_3O_7$. The key pre-requirement for short wavelength region is the extremely high $E_g$. In consequence, the accuracy in the calculation of $E_g$ is of great importance with respect to material designing and predicting their NLO properties. Although the plane wave-DFT method is an excellent way to predict the optical properties such as SHG coefficient, birefringence and phase matching, but the GGA as a correlation function usually severally underestimates the $E_g$.[4,5] To calculate the precise calculation of $E_g$, the non-local exchange hybrid functional (HSE06) as implemented in PWmat code is used because HSE06 offers much better description of $E_g$. Owing to the non-availability of the experimental $E_g$, so the difference between the two $E_g$-HSE06 and $E_g$ -GGA was used as a scissors operator for calculating the optical properties.

**Effect of Refractive Index Dispersion on PM Condition**

In NLO crystal, the ability of PM is the key because it regulates the applied shortest PM-SHG λ and SHG efficiency of the material. Dispersion of the refractive index is the crucial factor for PM in SHG. Small dispersion is preferred over large because it will provide short SHG λ.[6]

The linear optical properties were calculated by first principles calculation based on DFT with GGA and kept the default values of CASTEP on the aspects of the other calculation convergence criteria and parameters. The linear optical properties were calculated by dielectric function through following formula:

$$\varepsilon(\omega) = \varepsilon_1(\omega) + i\varepsilon_2(\omega)$$

Where $\varepsilon_1(\omega)$ is the real and $\varepsilon_2(\omega)$ are the imaginary dielectric function. The $\varepsilon_2(\omega)$ can be calculated by,

$$\varepsilon_2(\omega) = \frac{4\pi^2 e^2}{\Omega} \lim_{q\to 0} \frac{1}{q^2} \times \sum_{c,v,k} 2\omega_k \delta(E_c - E_v - \omega) \left| \left\langle c \left| e.q \right| v \right\rangle \right|^2$$

Where $\left| \left\langle c \left| e.q \right| v \right\rangle \right|$ presents the optical transition from the valance state ($v$) to conduction state (c). while e and q are the photon polarization direction and electron momentum operator respectively. On contrary, the real part of the dielectric function $\varepsilon_1(\omega)$ could be calculated from the imaginary part $\varepsilon_2(\omega)$ based upon the Kramers- Kroning transform and resultantly birefringence ($\Delta n$) and refractive index was calculated respectively.

Historically, the SHG coefficient calculation uses band theory which suffers from a sever explicit deviation in the static limit but according to Aspnes the divergent terms are vanished for cubic crystal.[7–9] Additionally, the Ghahramani *et al*. attain the divergence free general formulation by using the sum rule that improved through systematic separation of inter an intra band contribution.[10] Next, the Aversa and Sipe suggested the length gauge rather of velocity gauge to contribute expression which prevent from unphysical divergences.[11] Afterwards, the local field effect and general mixing frequency dependent formulation were proposed.[12–15] Currently, various approaches such as summation of state which is based on perturbation theory, density functional perturbation theory, wannier and Bloch orbital based theory and berry phase

method has been used to calculate the SHG coefficient.[10,16–21] However, in term of structural chemistry, the obtained SHG coefficient is not sufficient for distinguishing and identifying underlying response mechanism. Contribution identification from specific cation or anion group can be determined through the real space cutting through semi empirical parameters.[3,22] The particular bonds contribution assessed with localized bond charge model based on bonding characteristics.[23] Currently, the extended Bloch functions are usually used to calculate SHG response which arises from virtual electrons (VE), virtual hole (VH) process and two band transition process that later show exactly zero frequency. The static limit SHG coefficient,

$$\chi^2_{\alpha\beta\gamma} = \chi^2_{\alpha\beta\gamma}(VE) + \chi^2_{\alpha\beta\gamma}(HE)$$

The contribution of $V(E)$ and $V(H)$ are calculated by following Formula:

$$\chi^{(2)}_{\alpha\beta\gamma}(VE) = \frac{e^3}{2\hbar^2 m^3}\sum_{vcc'}\int\frac{d^3k}{4\pi^3}P(\alpha\beta\gamma)\,\mathrm{Im}\left[p^{a}_{cv}p^{\beta}_{cc'}p^{\gamma}_{c'v}\right]\times\left(\frac{1}{\omega^3_{cv}\omega^2_{vc'}}+\frac{2}{\omega^4_{vc}\omega_{c'v}}\right)$$

$$\chi^2_{\alpha\beta\gamma}(VH) = \frac{e^3}{2\hbar^2 m^3}\sum_{vv'c}\int\frac{d^3k}{4\pi^3}P(\alpha\beta\gamma)\,\mathrm{Im}\left[p^{a}_{vv'}p^{\beta}_{v'c}p^{\gamma}_{cv}\right]\times\left(\frac{1}{\omega^3_{cv}\omega^2_{v'c}}+\frac{2}{\omega^4_{vc}\omega_{cv'}}\right)$$

While $\alpha$, $\beta$ and $\gamma$ refer to the Cartesian components, $P(\alpha\beta\gamma)$, $p^{\alpha}_{ij}$ and $hw_{ij}$ denote the full permutation, momentum matrix element and band energy difference respectively; v/v and c/c are the valance and conduction bands respectively. The calculated SHG coefficient by means of this process is well matched with the experimentally calculated value when DFT- $E_g$ is corrected by scissor operator. The phenomenological anionic theory is suggested that the NLO effect is dominated by the contribution of anionic group in crystal.

In order to evaluate more instinctively demonstrated the electronic orbitals contribution towards the SHG effect, influence to the SHG coefficient of all the occupied and unoccupied band and SHG weighted-charge-density analysis scheme was summed up through the “band-resolved” scheme while the band charge density was determined by SHG weighted factor and visualized in the real space. Hence, the dominated orbitals contribution is displayed while those orbitals

which shows less contribution are not highlighted and the theoretical approaches have been used successfully to analyze the SHG coefficient of NLO crystal as mentioned in literature.[24,25]

**Table S1.** Properties of some borates based deep-ultraviolet nonlinear optical crystals.

| Crystal | Space group | $E_g$ (eV) | $\lambda_{UV}$ (nm) | $\Delta n$ (nm) | $\lambda_{PM}$ (nm) | SHG (× KDP) |
|---|---|---|---|---|---|---|
| $NaBe_2BO_3F_2$ | *C*2 | 8.07 | 154 | 0.091 at 200 | 185 | 1.40 |
| $KBe_2BO_3F_2$ | *R*32 | 8.45 | 147 | 0.077 at 1064 | 161 | 1.26 |
| $RbBe_2BO_3F_2$ | *R*32 | 8.18 | 152 | 0.073 at 1064 | 170 | 1.15 |
| $CsBe_2BO_3F_2$ | *R*32 | 8.23 | 151 | 0.058 at 1014 | 202 | 1.28 |
| $NH_4Be_2BO_3F_2$ | *R*32 | 8.12 | 153 | 0.057 at 400 | 174 | 1.20 |
| $NH_4B_4O_6F$ | $Pna2_1$ | 7.87 | 156 | 0.117 at 1064 | 158 | 3.0 |
| $CsBe_2B_3O_7$ **This work** | *R*32 | 6.45 | 192 | 0.108 at 1064 | 192 | 0.8 |

**Table S2.** Fractional Atomic Coordinates ($\times 10^4$) and Equivalent Isotropic Displacement Parameters ($Å^2 \times 10^3$) for 247622-ICSD. $U_{eq}$ is defined as 1/3 of the trace of the orthogonalised $U_{IJ}$ tensor.

| Atom | *x* | *y* | *z* | U(eq) | BVS |
|---|---|---|---|---|---|
| Cs1 | 0 | 0 | 0 | 11.23(18) | 1.319 |
| F1 | 0 | 0 | 7349.3(17) | 10.9(8) | 1.176 |
| O1 | 3096(10) | 0 | 5000 | 6.5(10) | 2.007 |
| Be1 | 0 | 0 | 8071(4) | 8.2(15) | 2.039 |
| B1 | 0 | 0 | 5000 | 4.4(16) | 2.976 |

The bond valance sum is calculated by bond-valance theory ($S_i = \exp[R_o\text{-}R_i/B]$, where $R_o$ is an empirical constant, $R_i$ is the length of the bond in angstroms), and $B = 0.37$).

**Table S3.** Fractional atomic coordinates ($\times 10^4$), equivalent isotropic displacement parameters ($Å^2 \times 10^3$) and the bond valence sum (BVS) for each atom in the asymmetric unit for $CsBe_2B_3O_7$. $U_{eq}$ is defined as 1/3 of the trace of the orthogonalised $U_{ij}$ tensor.

| Atom | *x* | *y* | *z* | U(eq) | BVS |
|---|---|---|---|---|---|
| B1 | 6666.7 | 3333.3 | 10785.5 | 0 | 2.737 |
| O4 | 0 | 0 | 7121.8 | 0 | 1.856 |
| Be17 | 0 | 0 | 8199.7 | 10.77 | 2.216 |
| O18 | 0 | 0 | 7780.5 | 35.64 | 1.939 |
| Cs | 0 | 0 | 0 | 45.76 | 1.005 |
| B29 | 0 | 0 | 5000 | 24.39 | 2.968 |
| O32 | -3120.9 | -0 | 5000 | 37.15 | 2.096 |

The bond valance sum is calculated by bond-valance theory ($S_i = \exp[R_o - R_i/B]$, where $R_o$ is an empirical constant, $R_i$ is the length of the bond in angstroms), and $B = 0.37$).

**Global Instability Index (GII)**

The Global Instability Index (GII) is used as a standard quantitative structural reliability parameter to verify chemical stability and distortion in the crystal. The GII can be calculated by,

$$GII = \frac{\sqrt{\sum_{i=1}^{N}\{(\sum_j S_{ij} - V_i)^2\}}}{N}$$

Where N is the number of atoms in the formula unit. The GII is calculated for CBBF and $CsBe_2B_3O$ as 0.139 and 0.147 respectively; both values are lower than 0.2, indicating the rationality of the structure.

**Table S4.** Interpretation of GII.

| GII Value | Structural Meaning |
|---|---|
| < 0.10 | Very stable and relaxed structure |
| 0.10 – 0.2 | Slight strain or negligible experimantal error |
| 0.20 – 0.3 | Noticable structural distortion |
| > 0.3 | Higly strained or incorrect structure |

In short,

Low GII = Stable and accurate structure

High GII = Disorder, highly stress and incorrect atomic positions

**Evolution of the Stability of $CsBe_2B_3O_7$**

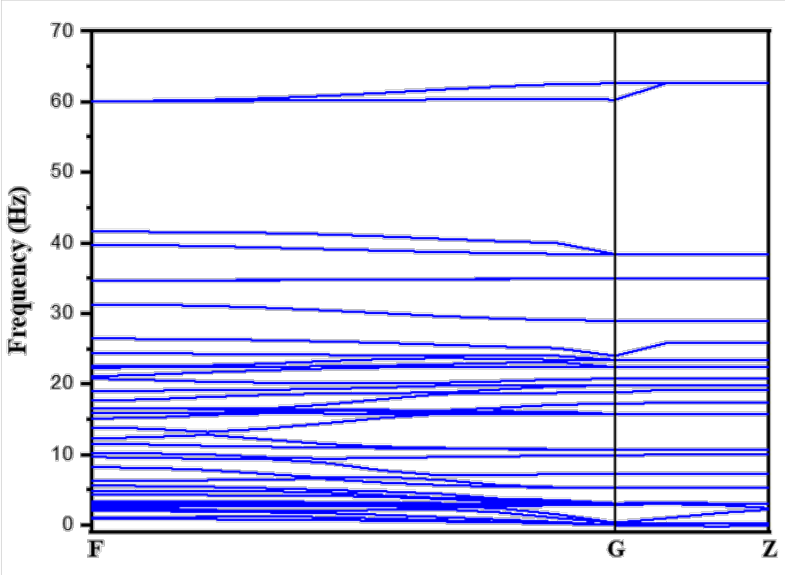


**Fig. S1:** Phonon dispersion spectra of $CsBe_2B_3O_7$.

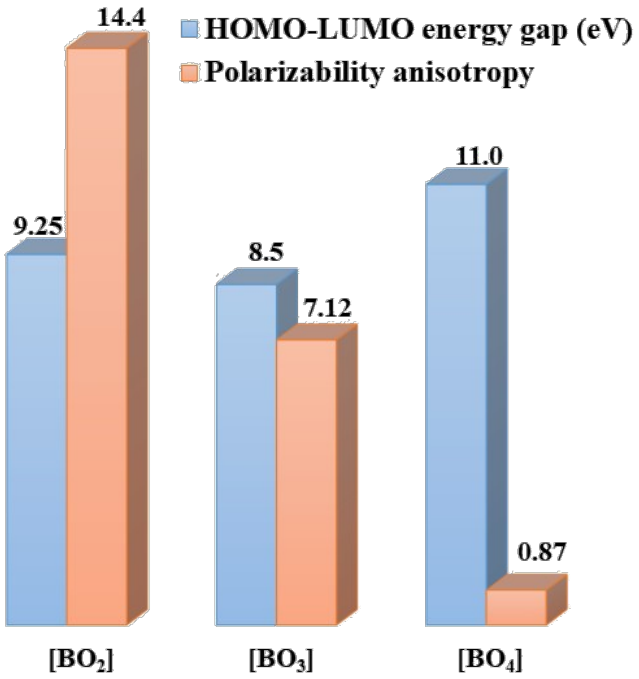


**Fig. S2:** Calculated HOMO LUMO gap and polarizability anisotropy of $[BO_2]$ and $[BO_3]$ units derived from our designed structure ($CsBe_2B_3O_7$) and $[BO_4]$ units from $LiB_3O_5$. The polarizability anisotropy of $[BO_2]$ unit is greater than $[BO_3]$ and $[BO_4]$ units, thus the large birefringence can be expected.

**Table S5.** Natural bond orbital summary.

| | NBO | Occupancy | Energy |
|---|---|---|---|
| | Molecular Unit Orbital | | |
| **1** | BD (1) B 1 - O 2 | 1.99936 | -0.72041 |
| **2** | BD (1) B 1 - O 3 | 1.99936 | -0.73537 |
| **3** | BD (2) B 1 - O 3 | 1.99904 | -0.06818 |
| **4** | BD (3) B 1 - O 3 | 1.99904 | -0.06818 |
| **5** | CR (1) B 1 | 1.9999 | -6.41649 |
| **6** | CR (1) O 2 | 1.99985 | -18.58035 |
| **7** | CR (1) O 3 | 1.99985 | -18.57786 |
| **8** | LP (1) O 2 | 1.96727 | -0.38896 |
| **9** | LP (2) O 2 | 1.72699 | 0.00995 |
| **10** | LP (3) O 2 | 1.72699 | 0.00995 |
| **11** | LP (1) O 3 | 1.96745 | -0.38436 |
| **12** | RY*(1) B 1 | 0.03218 | 0.70775 |
| **13** | RY*(2) B 1 | 0.00105 | 0.63501 |

| | | | |
|---|---|---|---|
| **14** | RY*(3) B 1 | 0 | 0.63431 |
| **15** | RY*(4) B 1 | 0 | 0.63431 |
| **16** | RY*(1) O 2 | 0.00096 | 1.27311 |
| **17** | RY*(2) O 2 | 0.00096 | 1.27311 |
| **18** | RY*(3) O 2 | 0.00057 | 1.20601 |
| **19** | RY*(4) O 2 | 0.0001 | 1.9173 |
| **20** | RY*(1) O 3 | 0.00102 | 1.27229 |
| **21** | RY*(2) O 3 | 0.00102 | 1.27229 |
| **22** | RY*(3) O 3 | 0.00057 | 1.2022 |
| **23** | RY*(4) O 3 | 0.0001 | 1.91717 |
| **24** | BD*(1) B 1 - O 2 | 0.01598 | 0.87937 |
| **25** | BD*(1) B 1 - O 3 | 0.01642 | 0.89363 |
| **26** | BD*(2) B 1 - O 3 | 0.27198 | 0.33824 |
| **27** | BD*(3) B 1 - O 3 | 0.27198 | 0.33824 |

**Table S6.** Bond distances and Mulliken population for characteristic atomic pair in $[BO_2]$, $[BO_3]$ and $[BeO_3F]$ in CBBF.

| Sr. No. | Value atom/pair | Bond distance (Å) | Bond population (e) |
|---|---|---|---|
| **1** | Be-F | 1.525 | 0.440 |
| **2** | Be-O | 1.632 | 0.390 |
| **3** | B-O | 1.374 | 0.820 |

**Table S7.** Bond distances and Mulliken population for characteristic atomic pair in $[BO_2]$, $[BO_3]$ and $[BeO_4]$ in $CsBe_2B_3O_7$.

| Sr. No. | Value atom/pair | Bond distance (Å) | Bond population (e) |
|---|---|---|---|
| **1** | B-O in $[BO_2]^-$ unit | 1.252-1.258 | 1.07-1.15 |
| **2** | B-O in $[BO_3]^{3-}$ unit | 1.374-1.375 | 0.810 |
| **3** | Be-O | 1.598-1.6 | 0.36-0.42 |

**Table S8.** Bond distances and Mulliken population for characteristic atomic pair in [$BO_3$] in $LiB_3O_5$.

| Sr. No. | Value atom/pair | Bond distance (Å) | Bond population (e) |
|---|---|---|---|
| **1** | B-O | 1.364-1.489 | 0.610-0.870 |

**References**


1 C. Chen, N. Ye, J. Lin, J. Jiang, W. Zeng and B. Wu, *Adv. Mater.*, 1999, **11**, 1071–1078.

2 S. J. Clark, M. D. Segall, C. J. Pickard, P. J. Hasnip, M. I. J. Probert, K. Refson and M. C. Payne, *Zeitschrift für Krist. - Cryst. Mater.*, 2005, **220**, 567–570.

3 C. Chen, Y. Wang, B. Wu, K. Wu, W. Zeng and L. Yu, *Lett. Nat.*, 1995, **373**, 1994–1996.

4 J. P. Perdew and Y. Wang, *Phys. Rev. B*, 1992, **45**, 13244–13249.

5 L. Xiong, J. Chen, J. Lu, C.-Y. Pan and L.-M. Wu, *Chem. Mater.*, 2018, **30**, 7823–7830.

6 Z. Yang, A. Tudi, B.-H. Lei and S. Pan, *Sci. China Mater.*, 2020, **63**, 1480–1488.

7 P. N. Butcher and T. P. McLean, *Proc. Phys. Soc.*, 1963, **81**, 219–232.

8 P. N. Butcher and T. P. McLean, *Proc. Phys. Soc.*, 1964, **83**, 579–589.

9 D. E. Aspnes, *Phys. Rev. B*, 1972, **6**, 4648–4659.

10 J. E. Sipe and E. Ghahramani, *Phys. Rev. B*, 1993, **48**, 11705–11722.

11 C. Aversa and J. E. Sipe, *Phys. Rev. B*, 1995, **52**, 14636–14645.

12 J. E. Sipe and A. I. Shkrebtii, *Phys. Rev. B*, 2000, **61**, 5337–5352.

13 Z. H. Levine, *Phys. Rev. B*, 1990, **42**, 3567–3577.

14 Z. H. Levine and D. C. Allan, *Phys. Rev. B*, 1991, **44**, 12781–12793.

15 J. Chen, L. Jönsson, J. W. Wilkins and Z. H. Levine, *Phys. Rev. B*, 1997, **56**, 1787–1799.

16 B. Zhang, M.-H. Lee, Z. Yang, Q. Jing, S. Pan, M. Zhang, H. Wu, X. Su and C.-S. Li, *Appl. Phys. Lett.*, 2015, **106**, 031906.

17 A. Dal Corso and F. Mauri, *Phys. Rev. B*, 1994, **50**, 5756–5759.

18 M. Veithen, X. Gonze and P. Ghosez, *Phys. Rev. B*, 2005, **71**, 125107.

19 D. Xiao, M.-C. Chang and Q. Niu, *Rev. Mod. Phys.*, 2010, **82**, 1959–2007.

20 R. D. King-Smith and D. Vanderbilt, *Phys. Rev. B*, 1993, **47**, 1651–1654.

21 D. Vanderbilt and R. D. King-Smith, *Phys. Rev. B*, 1993, **48**, 4442–4455.

22 K. Tsushima, A. Sibirtsev, A. W. Thomas and G. Q. Li, *Phys. Rev. C*, 1999, **59**, 369–387.

23 B. F. Levine, *Phys. Rev. B*, 1973, **7**, 2600–2626.

24 B.-H. Lei, Z. Yang, H. Yu, C. Cao, Z. Li, C. Hu, K. R. Poeppelmeier and S. Pan, *J. Am. Chem. Soc.*, 2018, **140**, 10726–10733.

25 F. Ding, W. Zhang, M. L. Nisbet, W. Zhang, P. S. Halasyamani, Z. Yang, S. Pan and K. R. Poeppelmeier, *Inorg. Chem.*, 2020, **59**, 759–766.